Electronic Supplementary Material (ESI) for Physical Chemistry Chemical Physics.

Novel two-dimensional tetragonal vanadium carbides and nitrides as promising materials for Li-ion batteries

Yi-Yuan Wu[a,b], Tao Bo[b,c], Junrong Zhang[b,c], Zhansheng Lu[d], Zhiguang Wang[e], Yuhong Li[a,*], and Bao-Tian Wang[b,c,f,*]

[a] *School of Nuclear Science and Technology, Lanzhou University, Lanzhou, 730000, China.*

[b] *Institute of High Energy Physics, Chinese Academy of Sciences (CAS), Beijing 100049, China.*

[c] *Dongguan Institute of Neutron Science (DINS), Dongguan 523808, China.*

[d] *College of Physics and Materials Science, Henan Normal University, Xinxiang 453007, China.*

[e] *Institute of Modern Physics, Chinese Academy of Sciences, Lanzhou 730000, China.*

[f] *Collaborative Innovation Center of Extreme Optics, Shanxi University, Taiyuan, Shanxi 030006, China.*

** Corresponding authors, E-mail: liyuhong@lzu.edu.cn, wangbt@ihep.ac.cn*

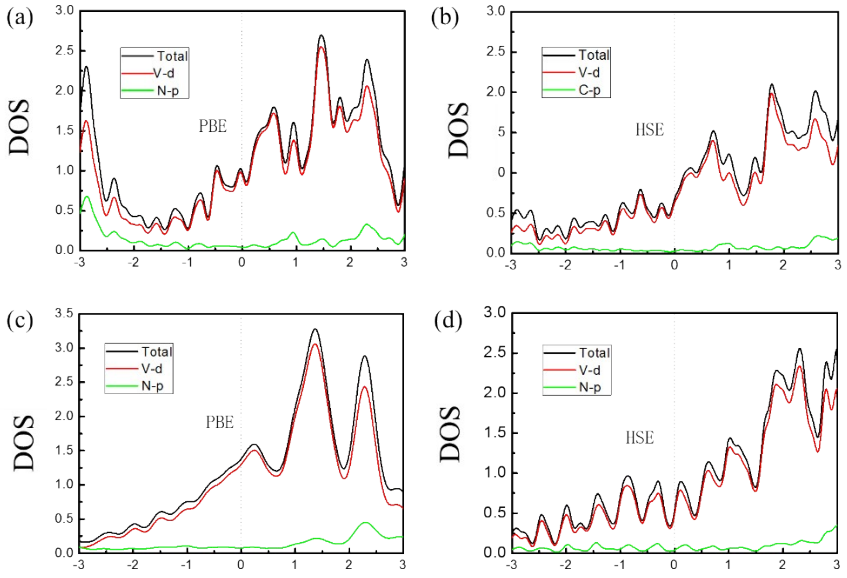

Fig. S1 Calculated DOS of (a) *tetr*-V_2C_2 and (c) *tetr*-V_2N_2 by PBE, and the DOS of (b) *tetr*-V_2C_2 and (d) *tetr*-V_2N_2 corrected by Heyd-Scuseria-Ernzerhof (HSE06) functional, where the Fermi energy is set to 0 eV.

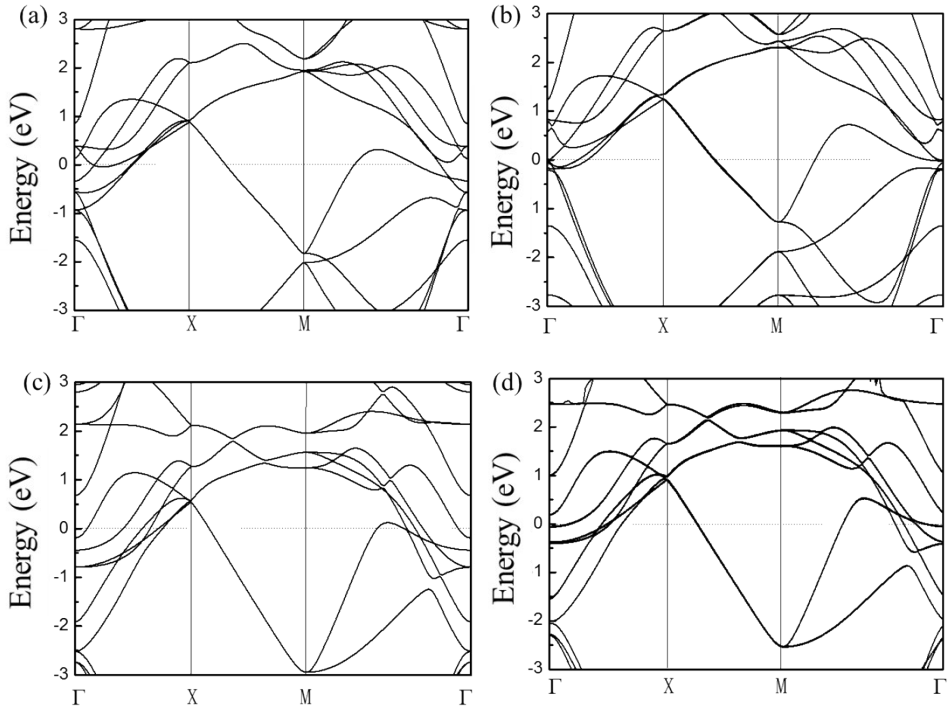

Fig. S2 Band structure of the monolayers (a) *tetr*-V_2C_2 and (c) *tetr*-V_2N_2 without the SOC effect, and the band structure of the monolayers (b) *tetr*-V_2C_2 and (d) *tetr*-V_2N_2 with the SOC effect, where the Fermi energy is set to 0 eV.

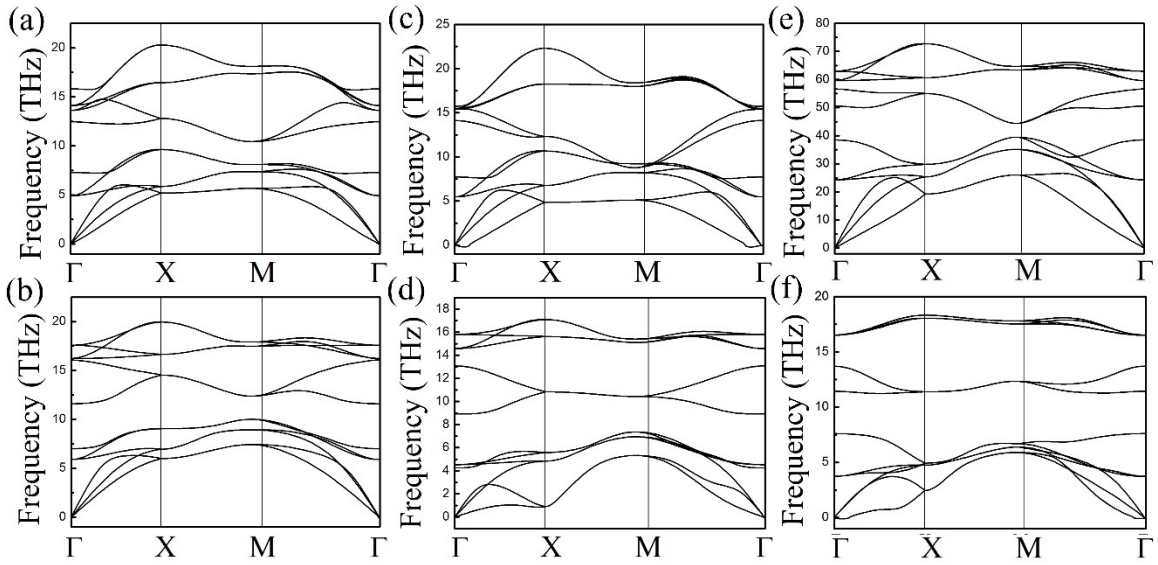

Fig. S3 Calculated phonon dispersion curves of the 2D (a) *tetr*-Ti_2C_2, (b) *tetr*-Ti_2N_2, (c) *tetr*-Zr_2C_2, (d) *tetr*-Zr_2N_2, (e) *tetr*-Nb_2C_2, (d) *tetr*-Nb_2N_2

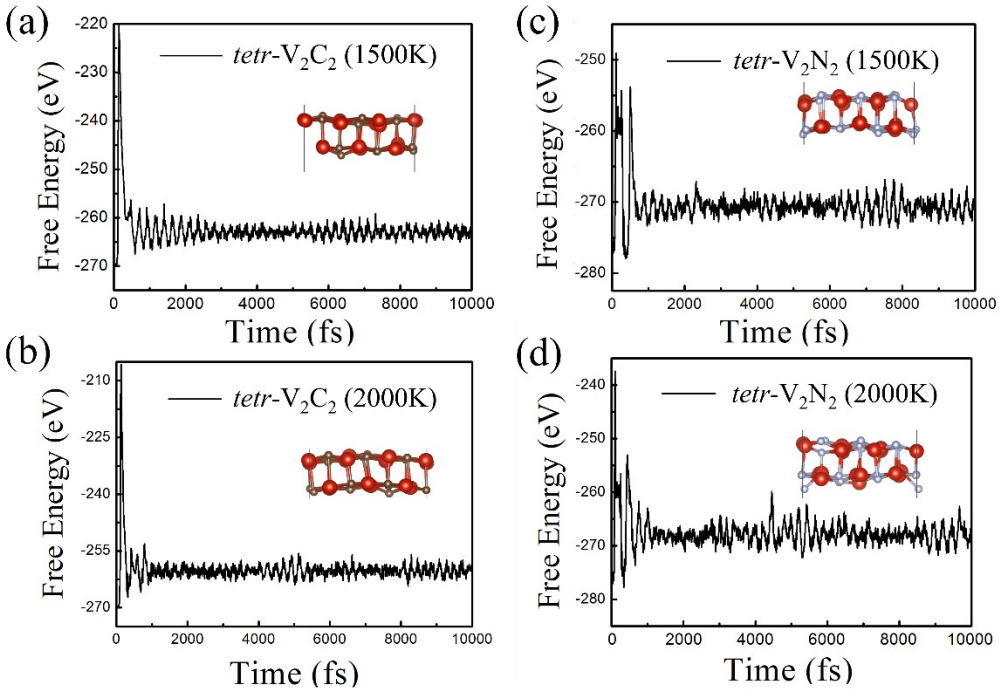

Fig. S4 Variation of the free energy of (a)/(b) *tetr*-V_2C_2 and (c)/(d) *tetr*-V_2N_2 in the AIMD simulations at 1500/2000K during the time scale of 10 ps. The trajectories of the structures are stable over the entire length of simulation time at 1500 and 2000 K. The illustrations denote snapshots for the equilibrium structures of corresponding structures at the temperatures of 1500 and 2000 K, at the end of 10000 fs AIMD simulations.

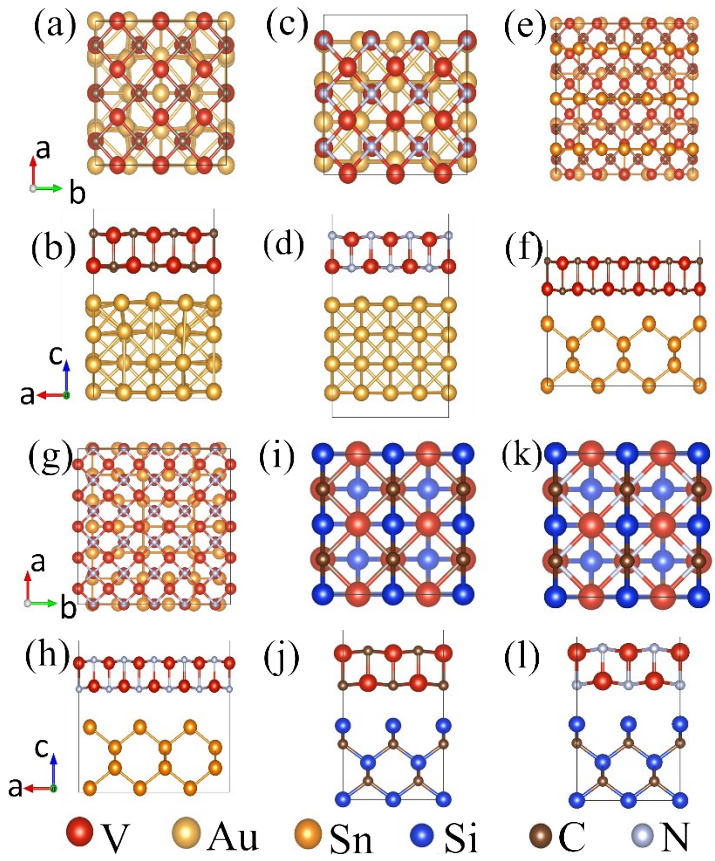

Fig. S5 Top views of the adsorption *tetr*-V_2C_2 (*tetr*-V_2N_2) on (a) Au (100), (e) Sn (100) and (i) SiC(100) [(c) Au (100), (g) Sn (100) and (k) SiC(100)]. The corresponding side views are given in the lower panels.

Table S1 Calculated lattice mismatch (δ) and adsorption energies (E_{ad}) for *tetr*-V_2C_2 and *tetr*-V_2N_2 on various substrates.

tetr-V_2C_2	δ (%)	E_{ad} (eV)	*tetr*-V_2N_2	δ(%)	E_{ad}(eV)
SiC(100)	-7.5	-7.35	SiC(100)	-9.5	-3.81
Au(100)	3.2	-5.49	Au(100)	5.0	-4.64
Sn(100)	3.5	-3.94	Sn(100)	3.0	-7.41

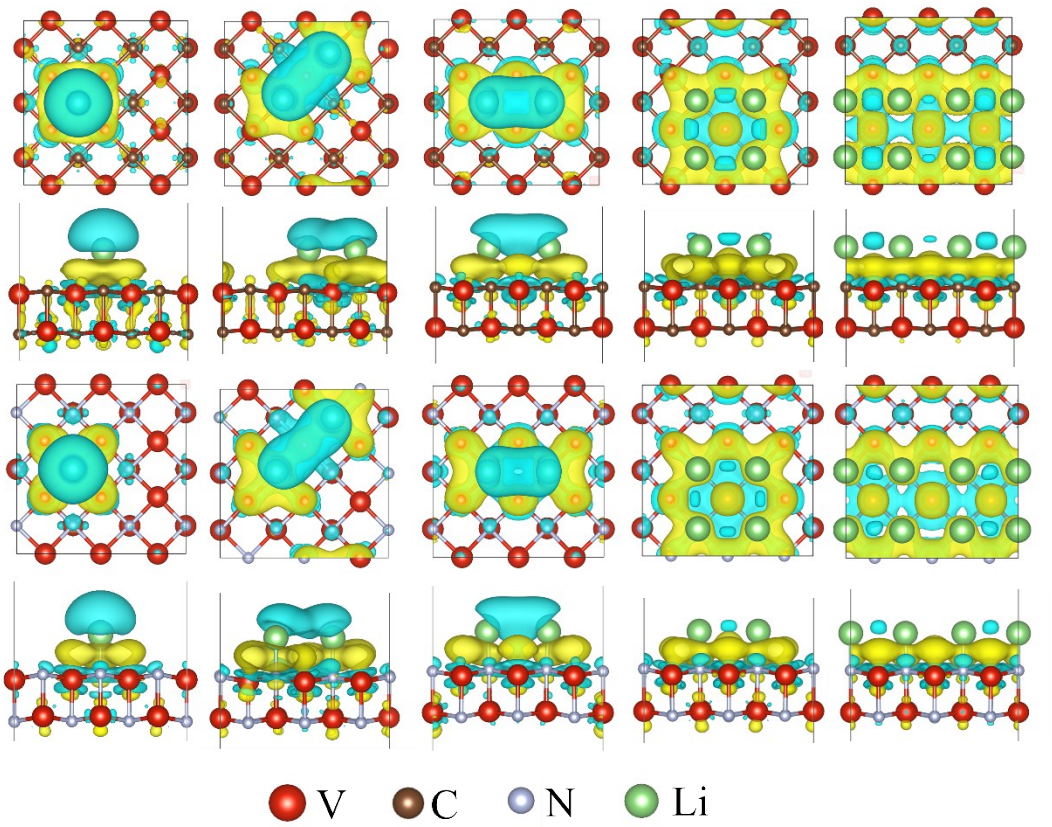

Fig. S6 The charge density difference plots of the single, double, quadra, and hexa-Li adsorbed on the *tert*-V_2C_2 and *tert*-V_2N_2. The yellow and blue areas denote electron gains and losses.

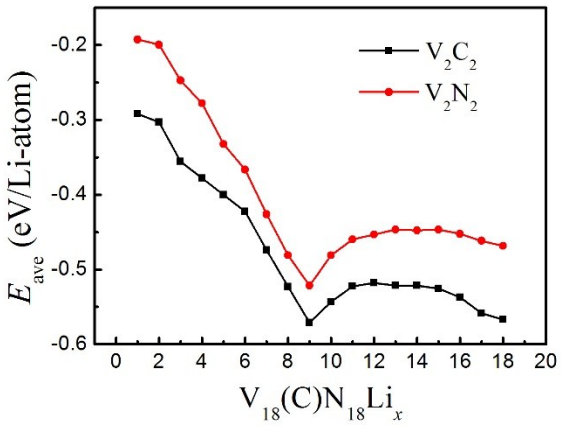

Fig. S7 Adsorption energies (E_{ave}) as the function of lithium concentration x in $V_{18}(C)N_{18}Li_x$.

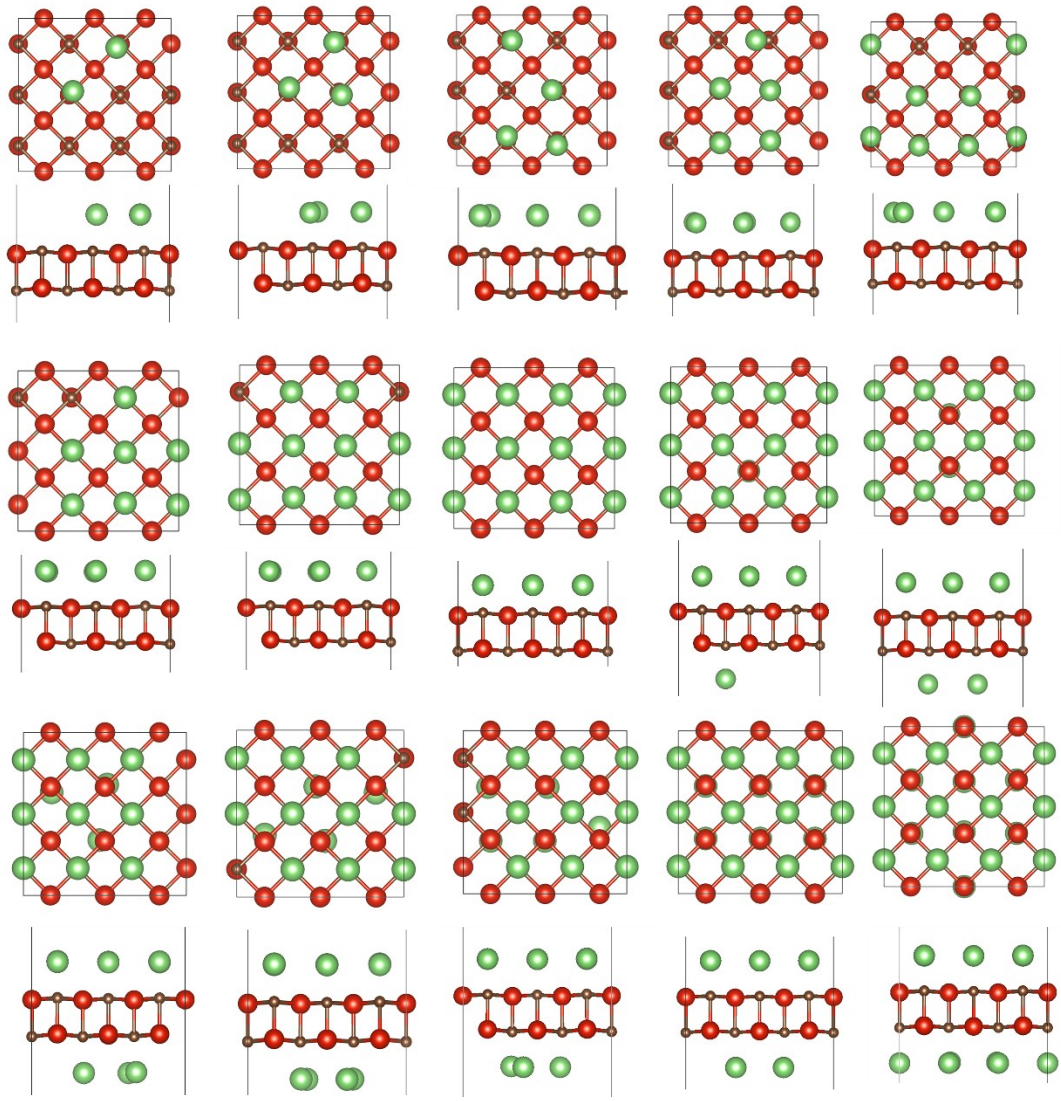

Fig. S8 Top and side views of the lowest adsorption energy configurations of *tert*-V_2C_2.

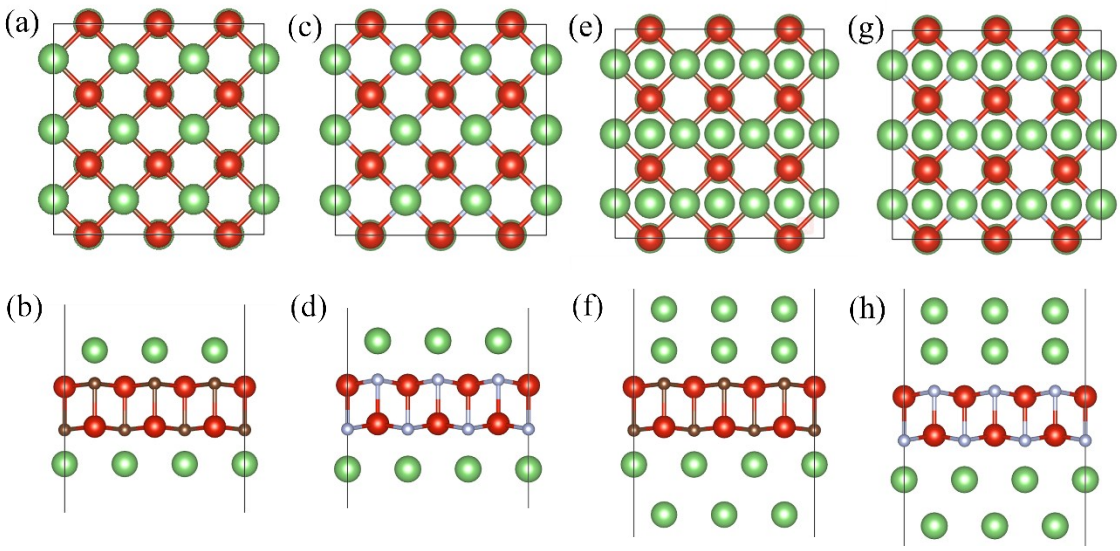

Fig. S9 Top and side views of the stable adsorption configuration of *tert*-V_2C_2 and *tert*-

V_2N_2 at $x = 1$ and 2.